Steering C–C Bond Cleavage and Hydrogenation in Polystyrene Hydrocracking through External Brønsted Acid Sites over Ni/Zeolites

Jonghyun Park [1,‡], Taeeun Kwon [1,‡], Ki Hyuk Kang [2], Wangyun Won [1,*], Insoo Ro [1,*]

[1] *Department of Chemical and Biological Engineering, Korea University, Seoul 02841, Republic of Korea*

[2] *Chemical & Process Technology Division, Korea Research Institute of Chemical Technology (KRICT), Daejeon 34114, Republic of Korea*

[‡] *These authors contributed equally.*

[*] *Corresponding Author:*

Prof. I. Ro (insooro@korea.ac.kr)

Table S1. Comparison of PS hydrocracking reactivity over acidic, non-acidic, and non-catalytic conditions.

Catalyst	Gas (wt%)	LOHC (wt%)	Liquid (wt%)	Solid residue (wt%)	Cyclic LOHCs / (aromatic+ cyclic LOHCs)	Hydrogen consumption (mmol)	Mass balance (%)
Ni/HY (30)	0.55	21.80	24.91	38.52	86.1	26.29	82.51
Ni/SiO_2	0.02	0.33	0.00	96.71	91.99	23.98	92.16
Ni/Al_2O_3	0.03	0.33	10.57	90.91	98.02	19.07	96.35
Ni/TiO_2	0.21	2.47	0.28	91.73	38.22	11.87	93.30
Blank [a]	0.01	0.69	1.61	90.44	1.14	5.79	91.43

Reaction conditions: 300 ℃, 6 h, 5% N_2/H_2, 3 MPa (at 25 ℃), 0.1 g of catalyst, 1.0 g of PS (M_w: ~192,000). [a] No catalyst.

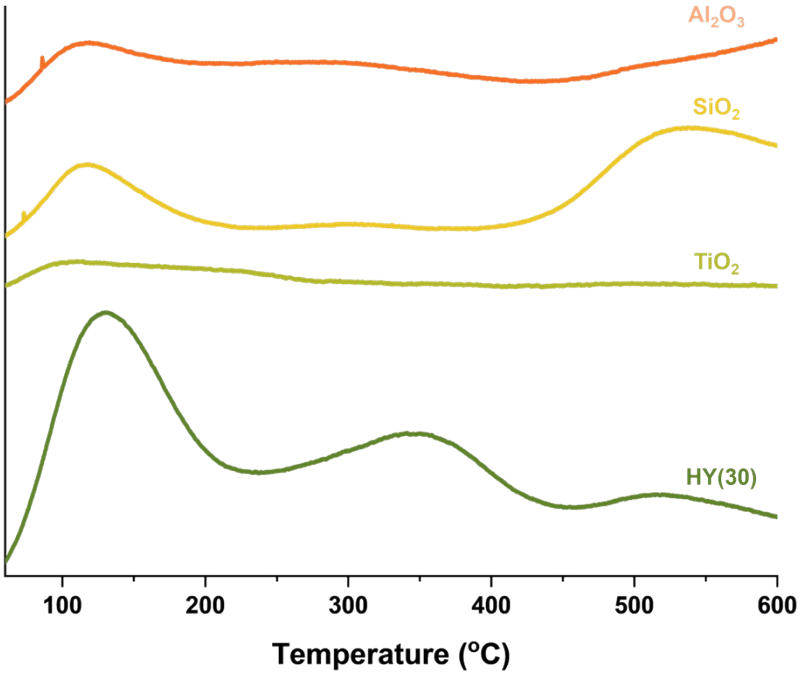

Figure S1. NH_3-TPD profile of Al_2O_3, SiO_2, TiO_2, and HY(30).

Table S2. Catalytic characterization results of different Ni/zeolite catalysts.

Catalyst	S_{BET} ($m^2 \cdot g^{-1}$)	S_{mic} ($m^2 \cdot g^{-1}$)	S_{ext} ($m^2 \cdot g^{-1}$)	Acid sites density [a] ($mmol \cdot g^{-1}$)			
				A_T	A_W	A_M	A_S
Ni/HY(30)	981.7	924.3	57.4	1.147	0.572	0.430	0.145
Ni/SiO_2	267.9	1.67	266.3	0.583	0.125	0.000	0.458
Ni/Al_2O_3	67.7	-	67.7	0.446	0.238	0.000	0.208
Ni/TiO_2	30.0	-	30.0	0.145	0.088	0.014	0.043

[a] Acid site density was determined by NH_3-TPD of the corresponding parent (metal-free) zeolites and was separated into A_T, A_W, A_M and A_S corresponding to the total, weak, medium, and strong acid sites, respectively.

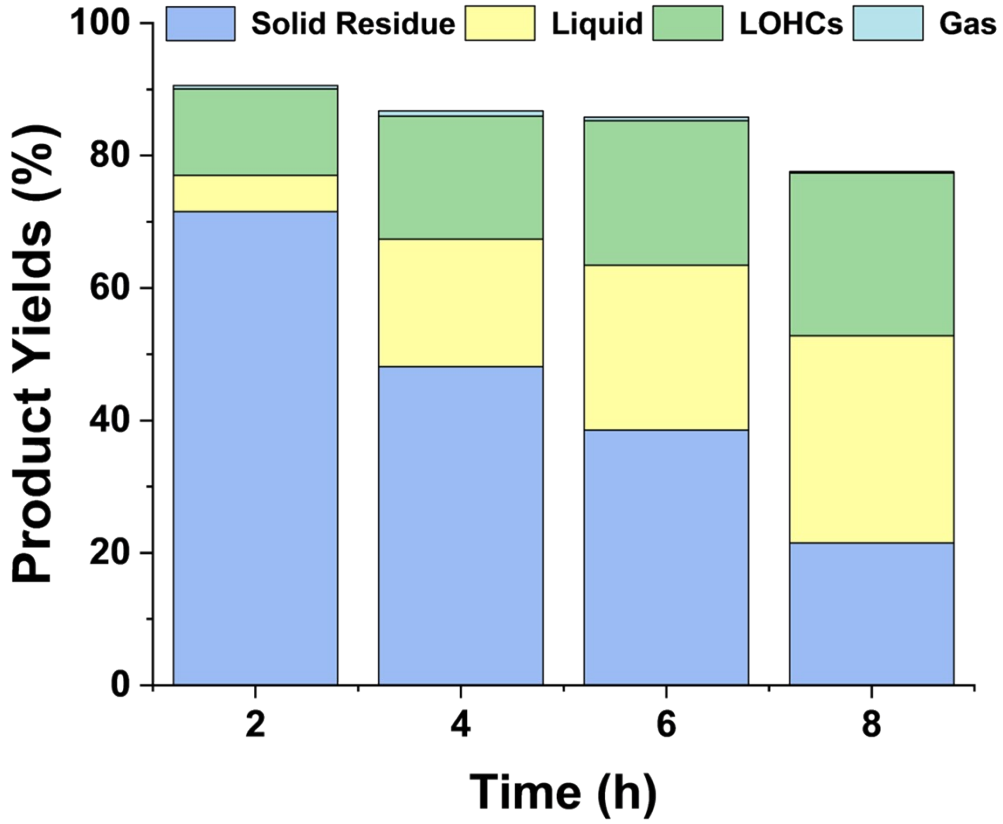

Figure S2. PS hydrocracking reaction results as a function of reaction time. Reaction conditions: 300 ℃, 5% N_2/H_2, 3 MPa (at 25 ℃), 0.1 g of Ni/HY(30), 1.0 g of PS (M_w: ~192,000).

Table S3. Effect of time, temperature and pressure on PS hydrocracking reactivity over Ni/HY(30) catalysts.

Reaction Condition	Gas (wt%[a])	LOHC (wt%)	Liquid (wt%)	Solid residue (wt%)	Cyclic LOHCs / (aromatic + cyclic LOHCs)	Hydrogen consumption (mmol)	Mass balance (%)
280 ℃	1.67	14.6	0.79	75.48	93.2	20.2	87.96
320 ℃	0.55	21.8	24.92	38.52	68.3	25.2	75.76
340 ℃	1.28	26.8	25.39	21.47	61.9	28.4	70.84
2 h	0.53	13.0	5.45	71.55	67.3	17.8	88.05
4 h	0.81	18.6	19.26	48.12	76.7	13.0	85.37
8 h	0.55	24.6	31.31	38.52	81.3	27.1	82.52
16 h	1.15	23.0	29.6	14.93	85.7	32.9	66.15
0.5 MPa	0.05	10.2	3.88	68.65	16.4	4.8	82.00
1 MPa	1.03	14.4	3.94	69.27	26.7	6.4	85.22
2 MPa	1.55	19.3	14.15	53.3	48.2	12.7	85.16
4 MPa	1.90	25.7	40.42	16.26	89.0	39.0	80.77

Unless otherwise noted, the reaction conditions were as follows: 300 ℃, 6 h, 5% N_2/H_2, 3 MPa (at 25 ℃), 0.1 g of Ni/HY(30), 1.0 g of PS (M_w: ~192,000).

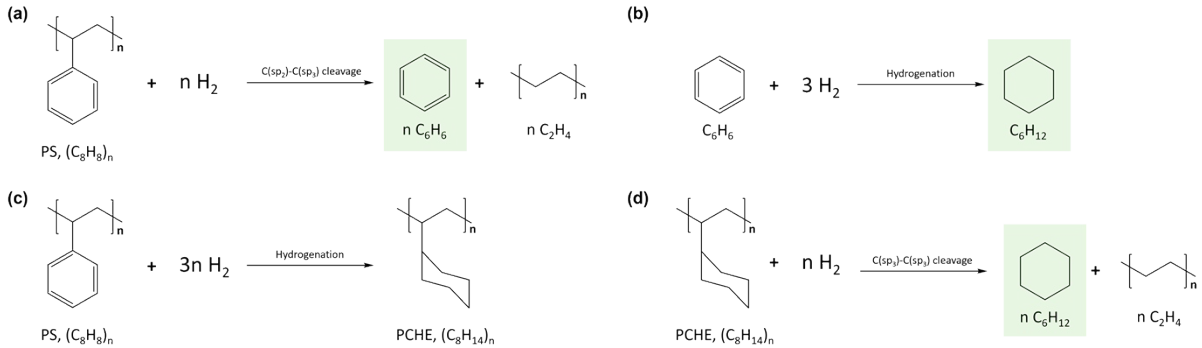

Figure S3. Schematic representation of possible formation pathways for major C_6 products from PS. (a) $C(sp^2)$–$C(sp^3)$ bond cleavage of PS. (b) Hydrogenation of benzene to cyclohexane. (c) Hydrogenation of PS to PCHE. (d) $C(sp^3)$–$C(sp^3)$ bond cleavage of PCHE.

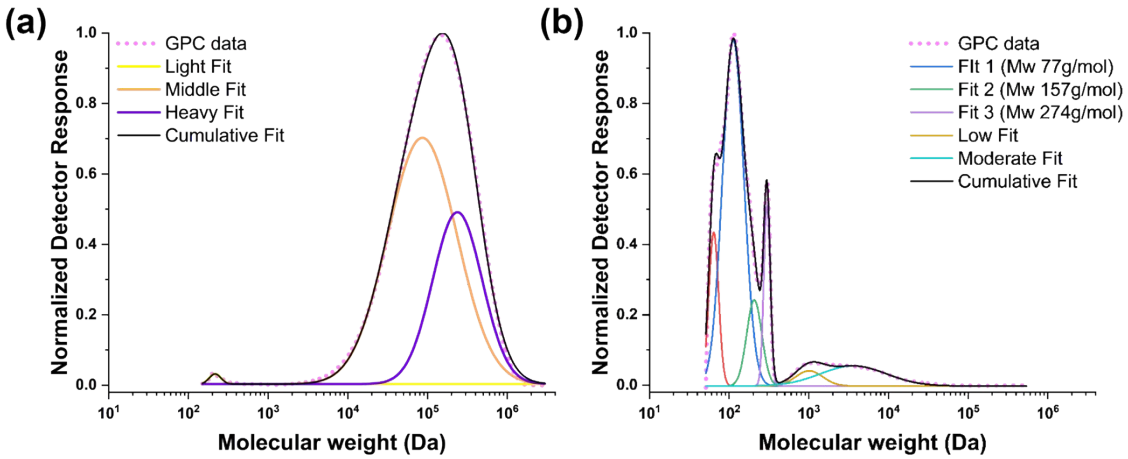

Figure S4. GPC molecular weight distributions of (a) pristine PS feed and (b) products obtained after PS hydrocracking over Ni/HY(30) under 300 °C, 4 MPa H_2, and 6 h.

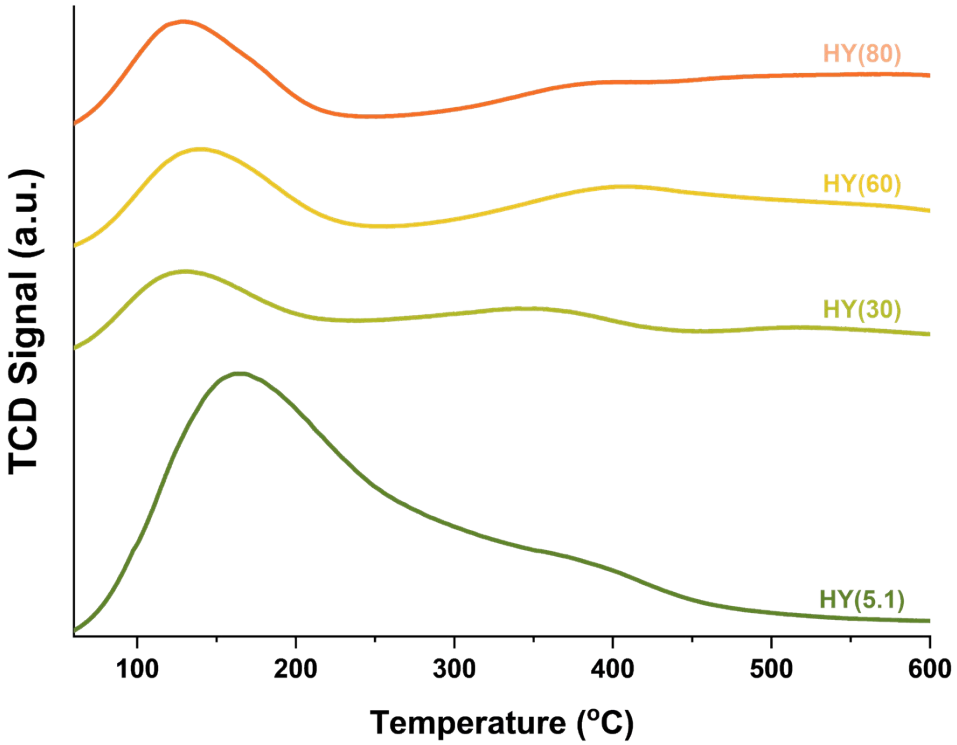

Figure S5. NH_3-TPD profile of HY zeolite with different SiO_2/Al_2O_3 ratios.

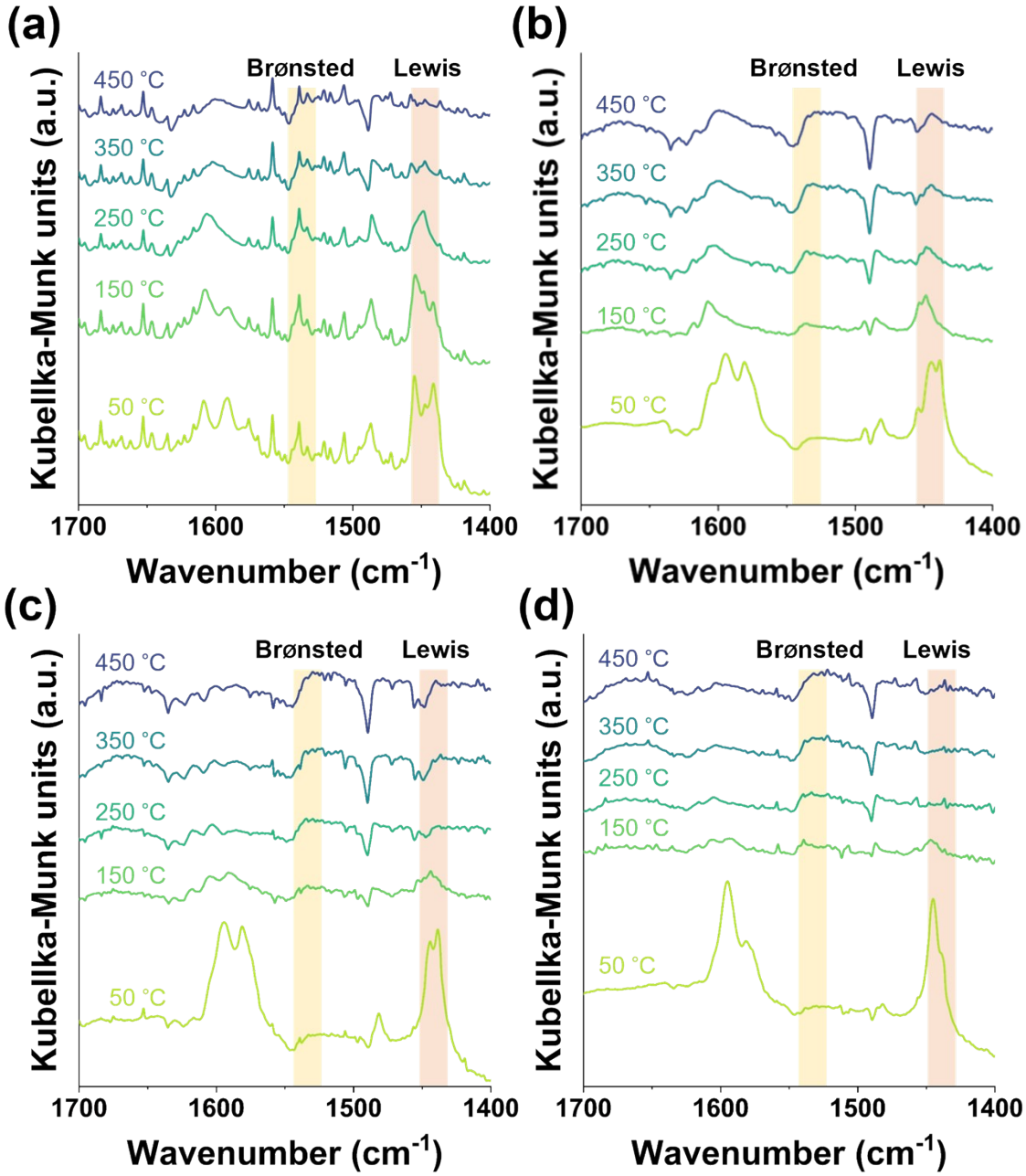

Figure S6. Pyridine-DRIFTS spectra of HY zeolite with different SiO_2/Al_2O_3 ratios. (a) Ni/HY(5.1), (b) Ni/HY(30), (c) Ni/HY(60) and (d) Ni/HY(80).

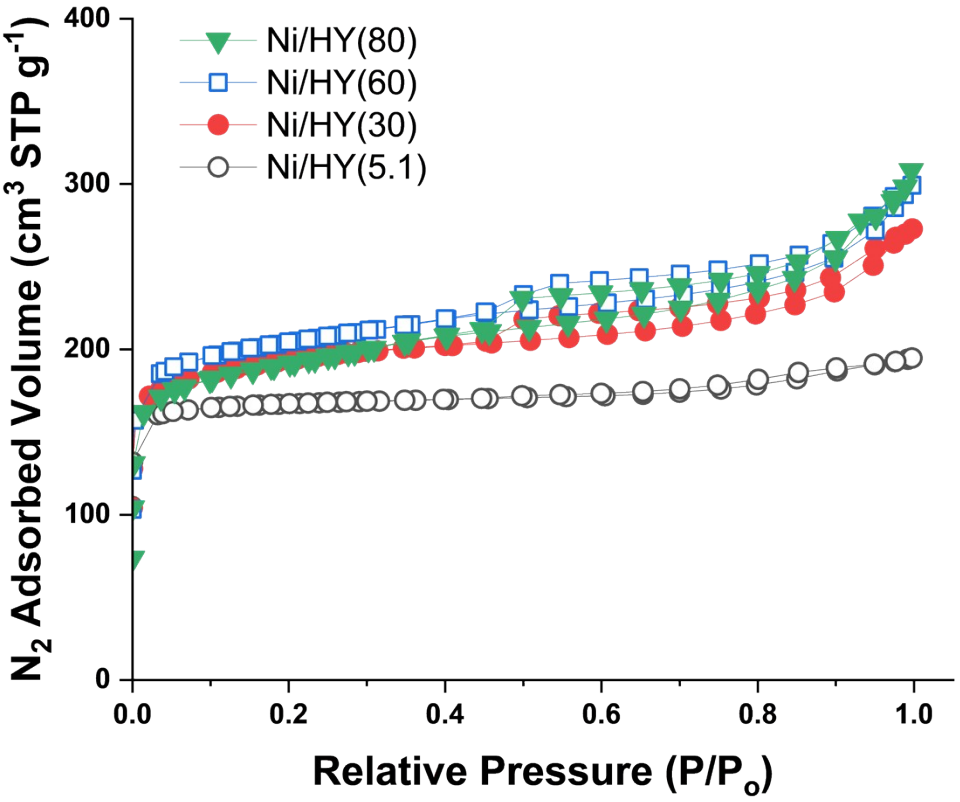

Figure S7. N_2 adsorption–desorption isotherms of HY zeolite with different SiO_2/Al_2O_3 ratios.

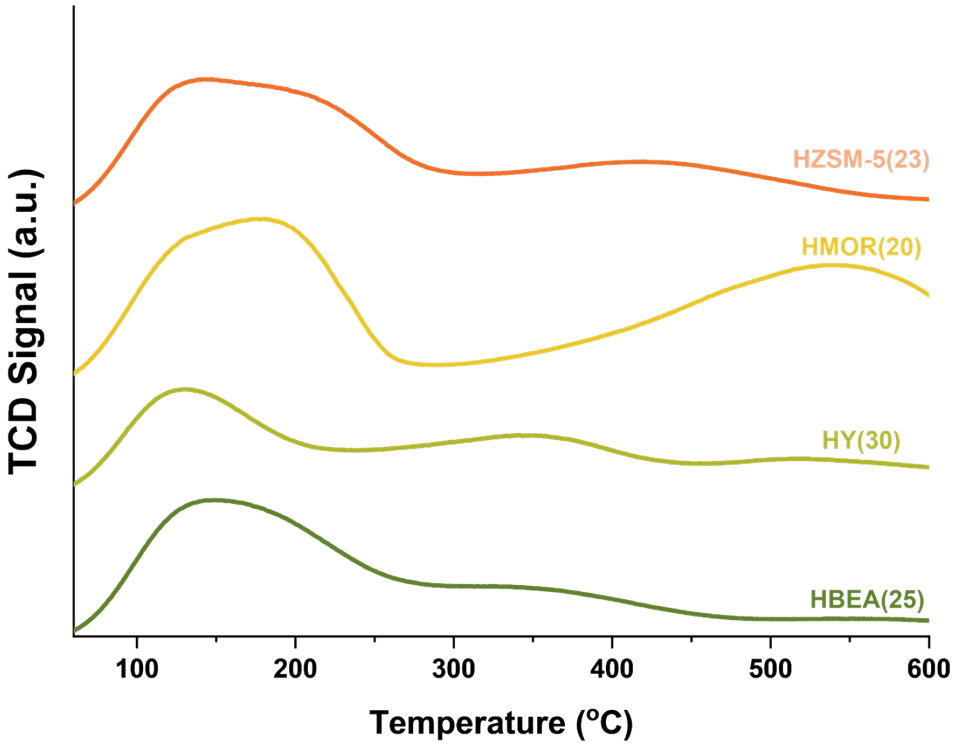

Figure S8. NH_3-TPD profile of different zeolites.

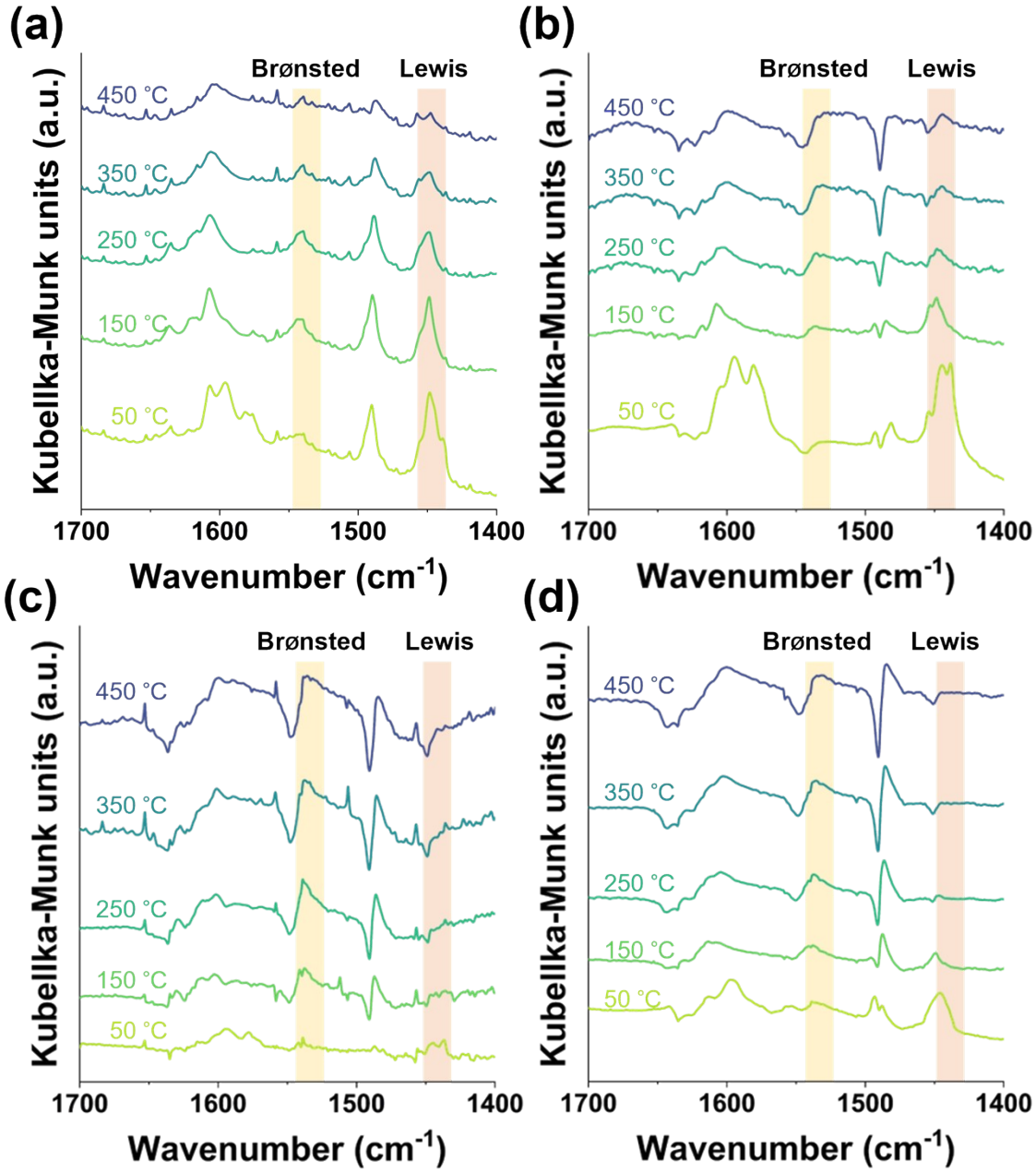

Figure S9. Pyridine-DRIFTS spectra of different zeolites. (a) Ni/HBEA(25), (b) Ni/HY(30), (c) Ni/HMOR(20) and (d) Ni/HZSM-5(23).

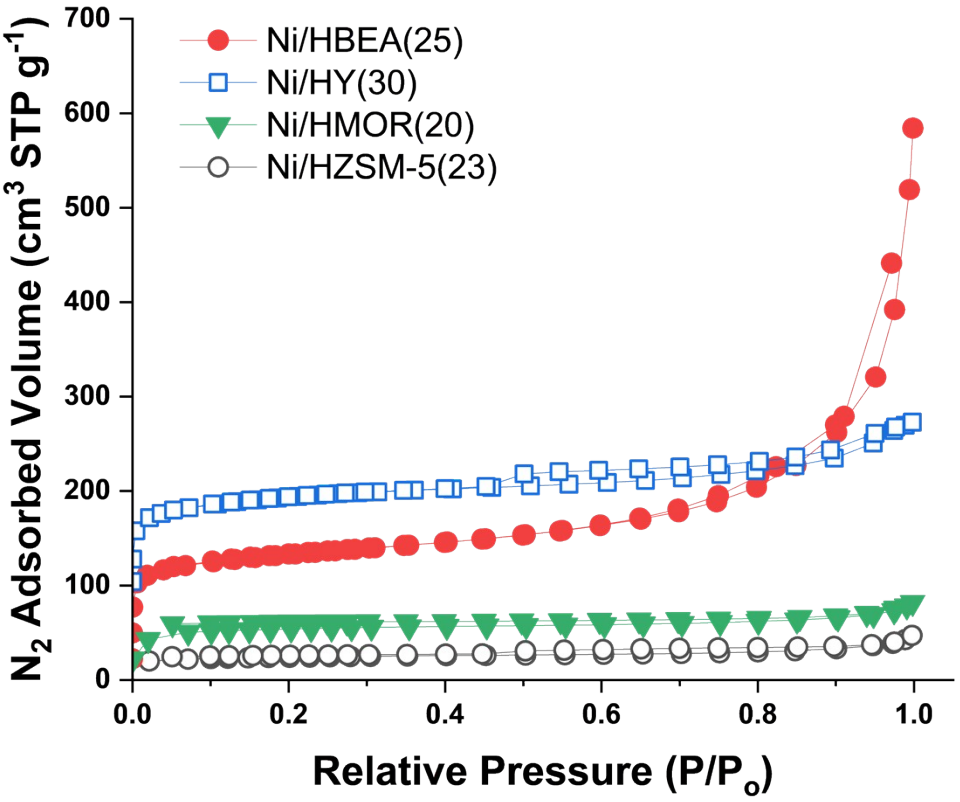

Figure S10. N_2 adsorption–desorption isotherms of different zeolites.

Table S4. Effect of PS hydrocracking over Ni catalysts with different acid properties

Catalyst	Gas (wt%)	LOHC (wt%)	Liquid (wt%)	Solid residue (wt%)	Cyclic LOHCs / (aromatic+ cyclic LOHCs)	Hydrogen consumption (mmol)	Mass balance (%)
Ni/HY(5.1)	2.00	4.22	3.24	85.53	70.3	21.6	93.62
Ni/HY(60)	2.65	17.04	17.43	52.75	95.8	22.6	88.04
Ni/HY(80)	0.25	12.32	9.94	66.98	92.4	18.4	86.53
Ni/HBEA(25)	0.37	25.04	45.39	8.87	88.81	33.6	75.44
Ni/HMOR(20)	0.29	12.14	13.68	54.61	37.80	12.3	80.85
Ni/HZSM-5(23)	5.85	5.91	0.00	80.82	16.06	20.9	80.79
Ni/HY(30)-pyridine	0.02	0.57	0.00	87.42	85.22	9.0	96.43
Ni/HY(30)-DTBP	0.00	0.63	0.00	98.99	88.47	5.7	93.58

Reaction conditions: 300 ℃, 6 h, 5% N_2/H_2, 3 MPa (at 25 ℃), 0.1 g of catalyst, 1.0 g of PS (M_w: ~192,000).

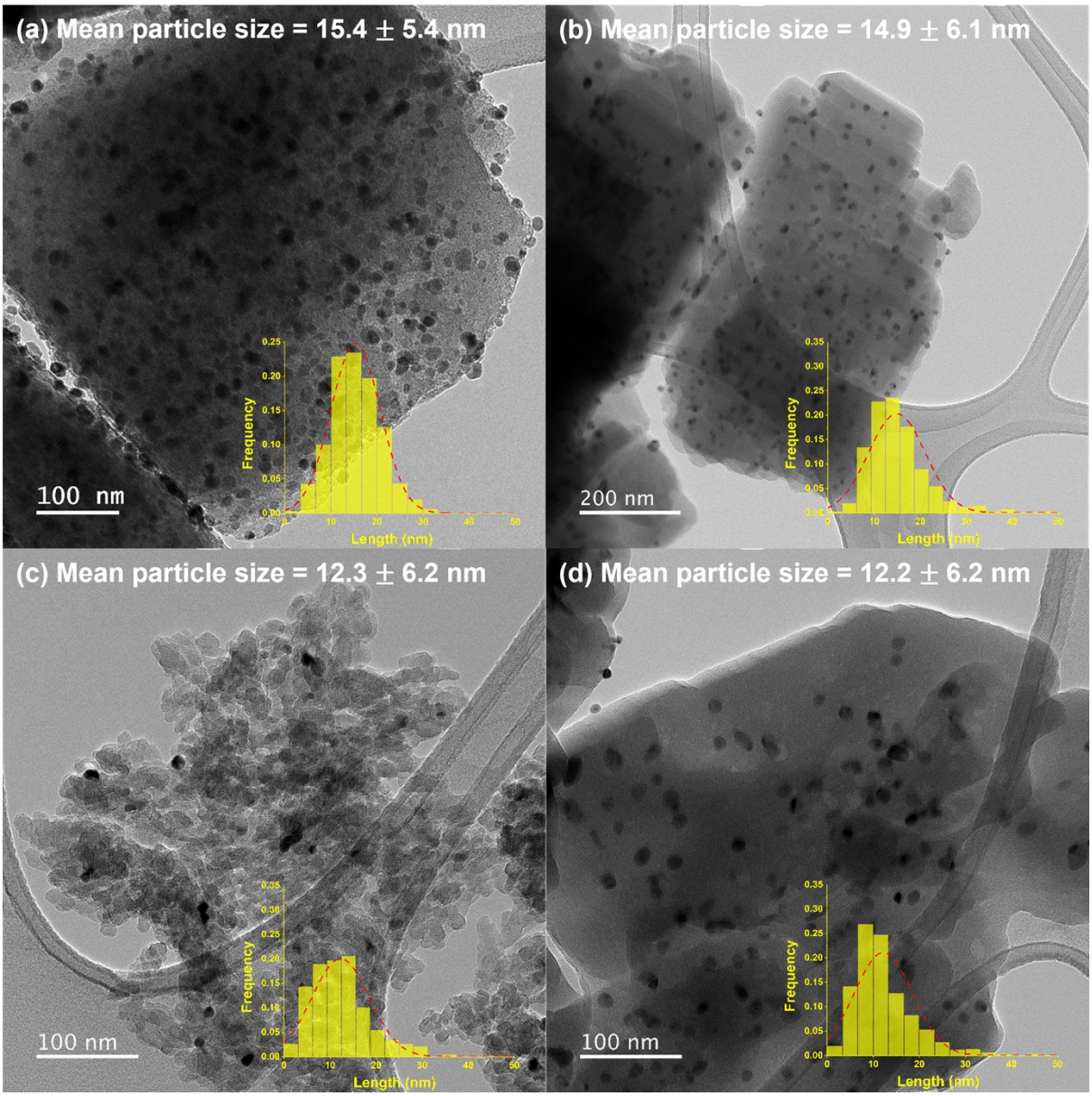

Figure S11. HRTEM images and corresponding particle size distribution histograms of (a) Ni/HY(30), (b) Ni/HZSM-5(23), (c) Ni/HBEA(25), and (d) Ni/HMOR(20).

Table S5. Crystallite size estimated from XRD analysis.

Catalyst	2θ range (°)	FWHM range	Scherrer Crystallite size (nm)
Ni/HY(5.1)	23.0–23.9	0.128–0.146	59.4
Ni/HY(30)	23.1–24.0	0.135–0.147	57.5
Ni/HY(60)	23.2–24.0	0.141–0.147	56.5
Ni/HY(80)	23.2–24.0	0.140–0.180	51.4
Ni/HBEA(25)	22.4–27.0	0.320–0.660	18.8
Ni/HMOR(20)	22.4–25.7	0.160–0.160	51.8
Ni/HZSM-5(23)	23.0–23.9	0.152–0.190	46.1

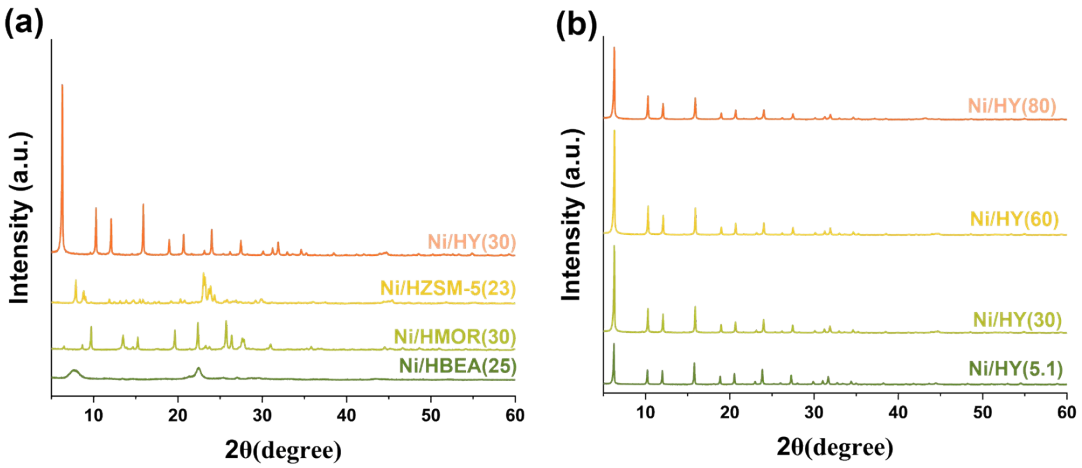

Figure S12. XRD patterns of (a) different zeolite catalysts and (b) catalysts with varying SiO_2/Al_2O_3 ratios.

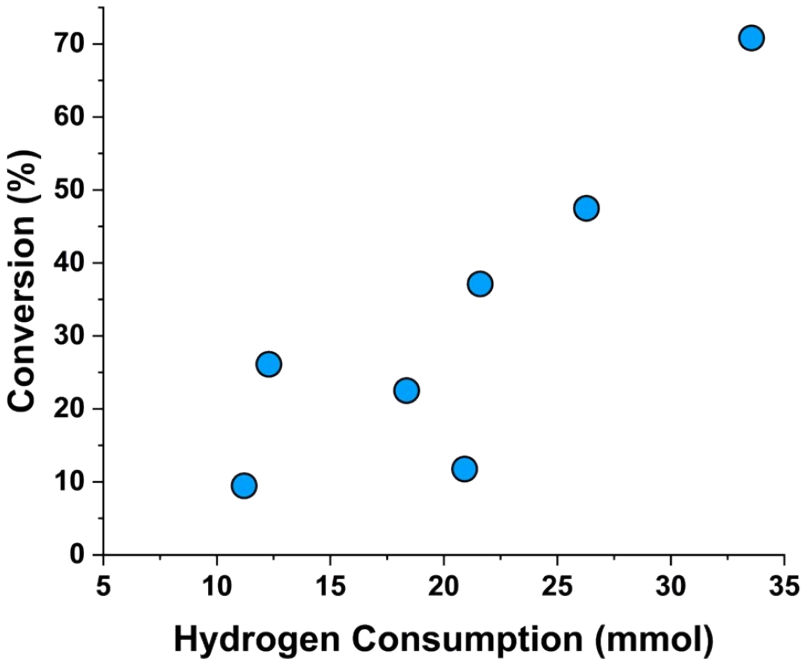

Figure S13. Correlation between PS conversion and hydrogen consumption amounts.